High-Speed Modulation of Index-Guided Implant-Confined Vertical-Cavity Surface-Emitting Lasers

Chen Chen, *Student Member, IEEE*, Paul O. Leisher, *Member, IEEE*, Daniel M. Kuchta, *Senior Member, IEEE*, and Kent D. Choquette, *Fellow, IEEE*

***Abstract*—An etched photonic crystal (PhC) or holey wedge structure induces index confinement into 850-nm implant-confined vertical-cavity surface-emitting lasers (VCSELs) to engineer the spatial overlap between the optical mode and laser gain for improved high-speed operation and reduced relative intensity noise. Large-signal operation of 12.5 Gb/s is achieved with a single transverse-mode PhC VCSEL and 15 Gb/s with a single transverse-mode holey VCSEL. An excessive current diffusion effect is found when the difference between the electrical and optical diameter is large (> 4 μm), which limits the large-signal modulation of single-mode VCSELs. The design rules for optimal single transverse-mode high-speed PhC and holey VCSELs are extracted from a parametric study of their large-signal modulation characteristics.**

***Index Terms*—High-speed modulation, semiconductor laser, vertical-cavity surface-emitting laser (VCSEL).**

I. Introduction

VERTICAL-CAVITY surface-emitting lasers (VCSELs) have emerged as dominant light sources for local-area network fiber optic data communication because of high-speed modulation, low power consumption, high-density 2-D array integration, and low manufacture cost. However, VCSELs tend to operate in multiple transverse modes. High-speed modulation of a single transverse-mode (a.k.a. single mode) VCSEL would be of interest not only for low dispersion data communication but also for other applications such as interrogation signals in optical sensing and atomic clocks. Multimode 10 Gb/s VCSELs are commercially available where direct modulation of VCSELs is pursued from different perspectives, which include optimizing epitaxial design [1]–[4], modifying device structure [5], [6], and improving thermal and modal management [7], [8].

Our approach to design a high-speed VCSEL is to stabilize its fundamental optical mode, and thus enable single-mode and high-speed operations simultaneously. The index guiding introduced by photonic crystals (PhCs) or holey wedge structures into implant-confined VCSELs has been shown to improve single-mode output, reduce threshold current, and improve laser efficiency and modulation bandwidth [6], [9]. The implementation of index confinement can be introduced independent of the electrical confinement, so the optical and gain diameters can be chosen for optimization of high-speed modulation. Note that our approach is independent of the epitaxial design, and thus, can be implemented into any wavelength regime or can augment other techniques for high-speed modulation operation.

The paper is organized as follows. In Section II, we describe the device structure and the dc properties, including the light–current–voltage (*LIV*), optical spectrum, and relative intensity noise (RIN) characteristics. In Section III, the modulation properties of the PhC and holey VCSELs are studied. For small-signal modulation, the maximum -3 dB bandwidth of 15 and 18 GHz have been achieved for the single-mode and multimode PhC VCSELs, respectively [6]. Large-signal operation of 12.5 Gb/s is achieved with a single-mode PhC VCSEL and 15 Gb/s with a single-mode holey VCSEL. It is shown that a PhC or holey wedge structure enables the independent tuning of the spatial overlap between the optical and ion-implanted aperture, and thus the spatial overlap between the fundamental optical mode and laser gain. Additionally, we observe a current diffusion effect under modulation operation, which becomes significant when the difference between the electrical and optical diameter is large (>4 μm), limiting the large-signal modulation of single-mode VCSELs. Lastly, the design rules to achieve high-speed single-mode PhC and holey wedge VCSELs are extracted, which provide guidance for determining the optical and ion-implanted apertures for optimized high-speed VCSELs.

II. Device Structure and DC Properties

The proton implant-confined VCSELs in this study were fabricated on wafers with conventional 850-nm epitaxy designs. Coplanar ground–signal–ground contacts were deposited on planarized low dielectric constant polyimide to reduce parasitic capacitance and facilitate on-wafer high-speed measurement [6]. The PhC and holey wedge structures were defined using electron beam lithography and etched approximately 16 periods (out of 21 total periods) into the top distributed Bragg reflector. Fig. 1 illustrates the device structure of a PhC and holey VCSEL. The PhC structure is determined by its lattice spacing a and hole diameter b [10], whereas the holey wedge structure is defined by its optical aperture radius R, the number

Manuscript received November 1, 2008; revised February 10, 2009. Current version published June 5, 2009.

C. Chen and K. D. Choquette are with the Department of Electrical and Computer Engineering, University of Illinois at Urbana-Champaign, Urbana, IL 61801 USA (e-mail: chenchen@uiuc.edu; choquett@illinois.edu).

P. O. Leisher is with nLight Corporation, Vancouver, WA 98665 USA (e-mail: paul.leisher@nlight.net).

D. M. Kuchta is with the IBM Thomas J. Watson Research Center, Yorktown Heights, NY 10598 USA (e-mail: kuchta@us.ibm.com).

Color versions of one or more of the figures in this paper are available online at http://ieeexplore.ieee.org.

Digital Object Identifier 10.1109/JSTQE.2009.2016115

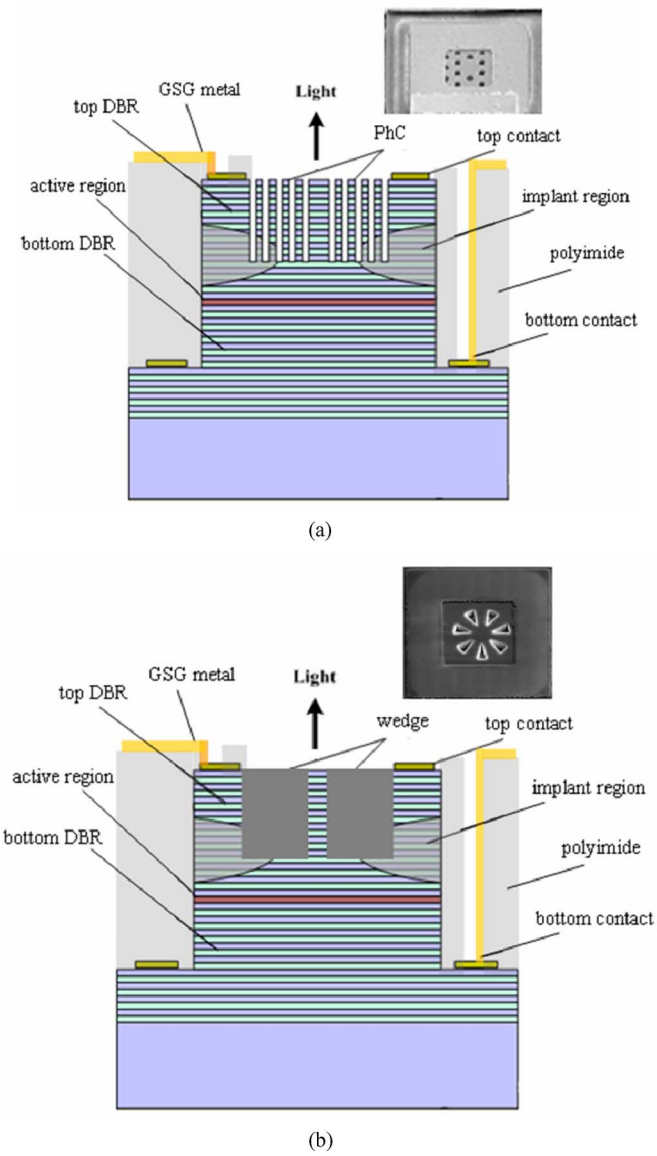

Fig. 1. Schematic of an implant-confined (a) PhC and (b) holey VCSEL. The insets are scanning electron micrographs of the laser facet with etched patterns.

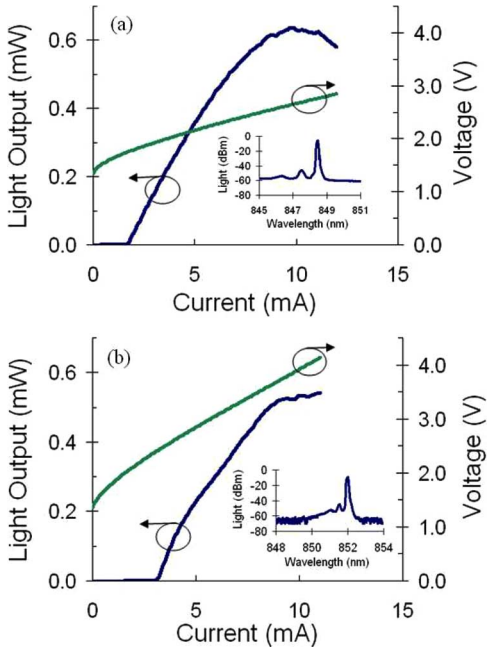

Fig. 2. *LIV* curves for (a) a single-mode PhC VCSEL with an 11-μm-diameter implant aperture, $a = 4$ μm, and $b/a = 0.7$ and (b) a single-mode holey VCSEL with a 10-μm-diameter implant aperture, $R = 4$ μm, $N = 7$, and $\theta = 20°$. The insets illustrate the optical spectrum of both devices at the maximum output power.

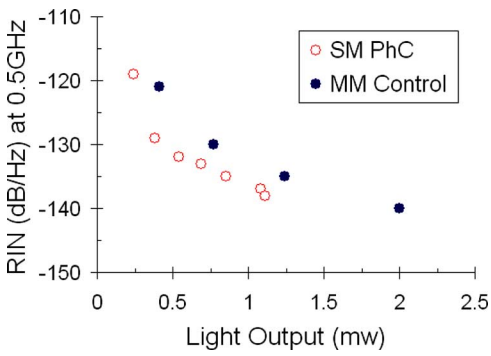

Fig. 3. Measured RIN at 500 MHz for a single-mode PhC VCSEL and a multimode VCSEL without PhC, where both devices have a 10-μm-diameter implant aperture.

of wedges N, and the angle subtended within each wedge arc θ [9].

The single-mode PhC VCSEL studied for large-signal operation has a 12-μm-diameter implant aperture, and $a = 4$ μm and $b/a = 0.7$, and the single-mode holey VCSEL studied for large-signal operation has a 10-μm-diameter implant aperture, $R = 8$ μm, $N = 7$, and $\theta = 20°$. The room-temperature continuous-wave (CW) *LIV* characteristics and optical spectrum for both devices are shown in Fig. 2. The PhC (and holey) VCSEL has a threshold current of 1.27 mA (and 3 mA), a slope efficiency of 0.269 W/A (and 0.127 W/A), and a series resistance of 139 Ω (and 250 Ω). In Fig. 3, we show the RIN characteristics for increasing output power, comparing a single-mode PhC VCSEL with a multimode VCSEL without an etched PhC pattern, but having the same implant aperture diameter. Although the same current density is expected for both VCSELs, only the carriers injected within the optical aperture of the PhC VCSEL can contribute to the laser optical mode. The RIN is measured using a 26-GHz spectrum analyzer. VCSEL output is coupled through free space optics and received by a 12-GHz photoreceiver with a gain of 26 dB. Fig. 3 illustrates that a single-mode PhC VCSEL generally produces lower RIN for a given light output power, which is due to higher photon density inside the cavity and lack of optical mode competition [11], [12]. However, the multimode conventional VCSEL can achieve lower overall RIN due to a larger rollover current and higher maximum optical power.

III. Modulation Properties

In our modulation measurements, a cleaved 50/125-μm graded-index multimode fiber and a high-speed photodector are

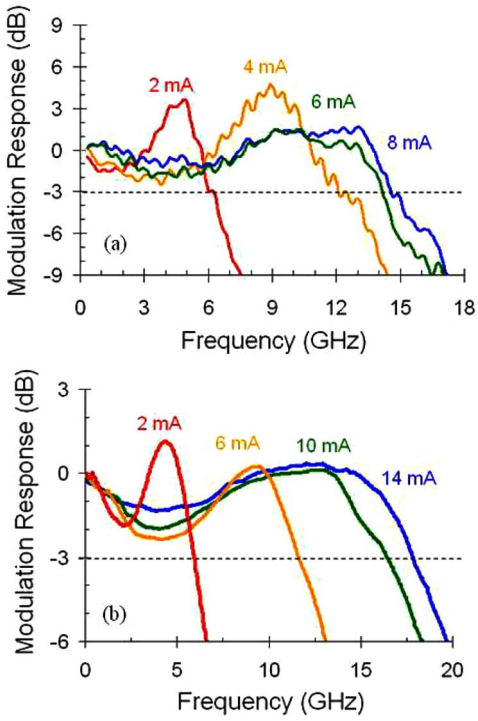

Fig. 4. Small-signal modulation response at several current injection levels. (a) Single-mode PhC VCSEL with maximum -3 dB modulation bandwidth of 15 GHz. (b) Multimode PhC VCSEL with maximum -3 dB bandwidth of 18 GHz.

used to collect output light from the VCSEL under test. For the small-signal modulation, the modulation voltage is supplied from a network analyzer via a 40-GHz ground—signal–ground microwave probe. For the large-signal modulation, the modulation voltage is supplied by a pattern generator producing a nonreturn to zero pseudorandom bit sequence of $2^7 - 1$.

A. Small-Signal Modulation

Fig. 4 shows the small-signal modulation response of a single-mode and multimode implant-confined PhC VCSEL at a variety of current injection levels. For the single-mode device, the maximum modulation bandwidth of 15 GHz is achieved at 8 mA in Fig. 4(a). This single-mode PhC VCSEL has an implant diameter of 11 μm, and PhC parameters of $b/a = 0.7$ and $a = 4$ μm. This laser has a threshold current of 1.35 mA, a slope efficiency of 0.26 W/A, a series resistance of 137 Ω, and maintains stable fundamental mode operation through rollover. The maximum modulation bandwidth of a multimode device is 18 GHz, as shown in Fig. 4(b). This multimode PhC VCSEL shows two dominate transverse modes and has an implant diameter of 12 μm, and PhC parameters of $b/a = 0.4$ and $a = 4.5$ μm. This laser has a threshold current of 1.35 mA, a slope efficiency of 0.38 W/A, and a series resistance of 102 Ω. The larger optical cavity ($2a - b$) of the latter VCSEL leads to multimode operation, but the lower series resistance and higher photon density produce higher bandwidth compared to the single-mode VCSEL. Note that the small-signal responses in Fig. 4(a) and (b) are measured with different average and smooth factors.

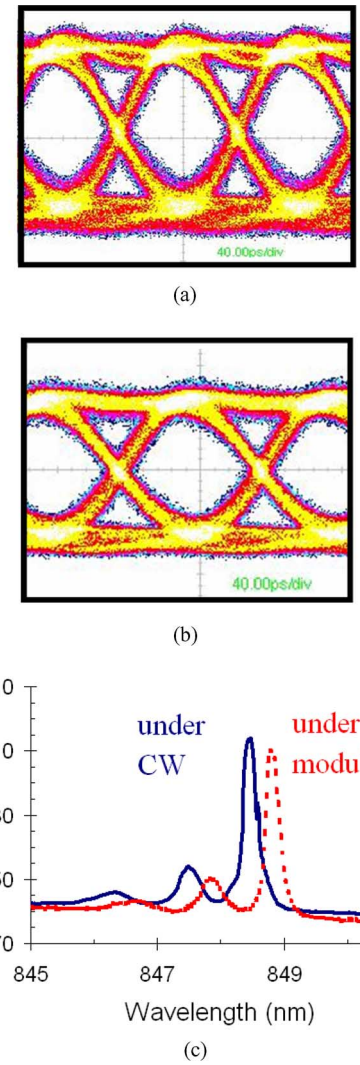

Fig. 5. Eye diagram for (a) PhC VCSEL operating at 12.5 Gb/s and (b) holey VCSEL operating at 15 Gb/s. (c) Optical spectrum of the PhC VCSEL in (a) under CW (solid line) and 12.5 Gb/s modulation (dash line) with a dc current of 7 mA.

B. Large-Signal Modulation

Fig. 5(a) illustrates the eye diagram of the single-mode PhC VCSEL in Fig. 2(a) operating at 12.5 Gb/s. This large-signal modulation is obtained with a current bias of 7 mA and a peak–peak modulation voltage of 1 V. The resulting extinction ratio is 4.94 dB and rms jitter is 6.76 ps. The 10%–90% rise time and fall time are 33 and 49 ps, respectively. Fig. 5(b) illustrates the eye diagram of the holey VCSEL in Fig. 2(b) operating at 15 Gb/s. This large-signal modulation is obtained with a current bias of 9.5 mA and a peak–peak modulation voltage of 1.3 V. The measured extinction ratio is 4.77 dB and rms jitter is 2.72 ps. The 10%–90% rise time and fall time are 31 and 37 ps, respectively. The single-mode devices consistently exhibit a slightly longer fall time than rise time. The transition tail tends to encroach into the timing window of the next bit, which deteriorates the eye quality. Fig. 5(c) illustrates the optical spectrum for the single-mode PhC VCSEL under CW (with current bias of 7 mA) and

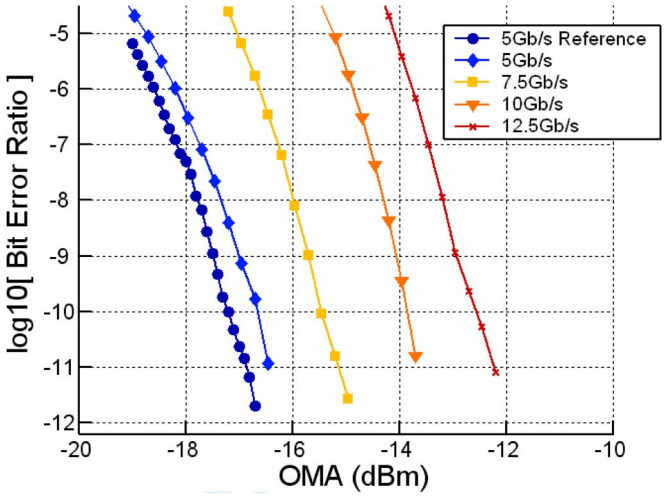

Fig. 6. Back-to-back BER versus OMA for the single-mode holey VCSEL in Fig. 2(b) at different bit rates. Receiver sensitivity limit is shown by the 5 Gb/s reference curve.

under the 12.5 Gb/s modulation. The single-mode operation with greater than 35 dB side-mode suppression ratio (SMSR) is attained with the use of PhC. The spectrum slightly shifts to longer wavelength because of device heating under high-speed modulation.

Fig. 6 illustrates the bit error ratio (BER) curves for the single-mode holey VCSEL at different bit rates under a back-to-back condition. The VCSEL is biased at 9.5 mA during the tests under different bit rates. One of the BER curves at 5 Gb/s is obtained using a reference laser transmitter to measure the receiver sensitivity limit, and the receiver has a bandwidth of 12 GHz. The minimum optical modulation amplitude (OMA) to achieve a BER $< 10^{-12}$ at 5 Gb/s is -16 dBm, which increases with increasing data rate to compensate for the deteriorating eye patterns.

C. Diffusion Capacitance Model

A trend is observed that the multimode PhC VCSEL and single-mode holey VCSELs generally produce better open eyes than the single-mode PhC VCSELs, especially when they are operating at bit rates beyond 10 Gb/s. The limitation for large-signal modulation of the single-mode PhC VCSELs can be attributed to a slow carrier diffusion mechanism [13]. The slow carrier effect is more prominent in the PhC VCSELs due to the larger difference in dimension between the optical aperture that is defined by PhC and the electrical current aperture defined by ion implantation. For the PhC VCSEL in Fig. 2(a), the diameter of the optical aperture is 6.8 μm smaller than that of the electrical current aperture, whereas this difference is 2 μm for the holey VCSEL in Fig. 2(b). Thus, the electrical current in the PhC VCSEL tends to experience an additional electrical parasitic effect as carriers diffuse toward the optical mode over a longer distance, as depicted in Fig. 7.

Fig. 8 illustrates the measured rise time of PhC and holey VCSELs determined from examination of the unfolded large-signal modulation data. The 10%–90% rise time is measured

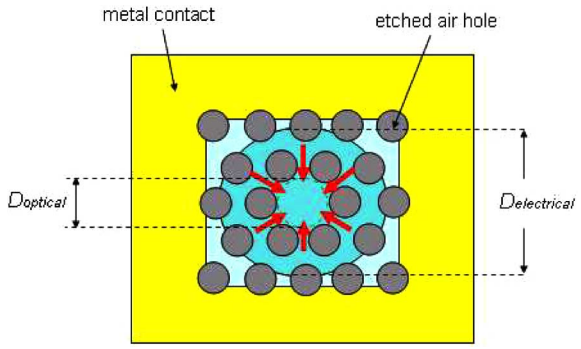

Fig. 7. Sketch of carrier diffusion in a PhC VCSEL. The arrows indicate that charge carriers diffuse toward the optical mode(s) confined within the optical aperture.

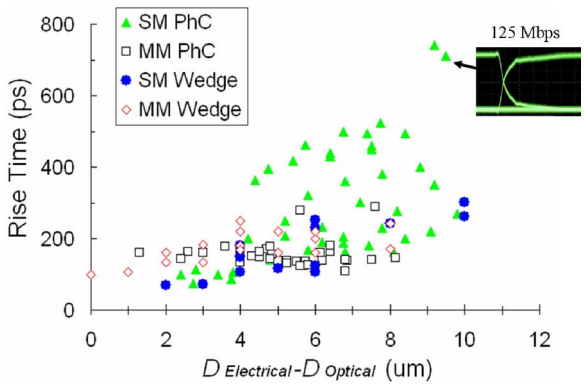

Fig. 8. Measured rise time as a function of diameter difference between the electrical and optical aperture for PhC and holey VCSELs under 125 Mb/s modulation. The inset shows an output pulse for 125 Mb/s modulation.

at 125 Mb/s where the large-signal eyes are fully open and is optimized for each device by varying the injection current. The diameter difference in Fig. 8 is the difference between the electrical aperture $D_{\mathrm{Electrical}}$ (defined by ion implantation) and the optical aperture D_{Optical} (defined by the PhC defect or the holey wedges), the latter being equal to $2a - b$ and $2R$ for the PhC and holey VCSEL, respectively. Evident in Fig. 8 is the rise time decreases as the aperture size difference becomes smaller. Note that the similar trend should also be expected for the fall time. This is because charge carriers diffuse across shorter lateral distance inward to support the optical mode(s) (see Fig. 7), resulting in less electrical parasitics. A laser with shorter rise time will produce superior open eyes at high bit rates. The fastest single-mode PhC VCSEL with >5 dB extinction ratio, as shown in Fig. 2(a), is limited to 12.5 Gb/s due to the large aperture size difference. For a very large aperture diameter difference, the electrical parasitic effect is pronounced even at low bit rates such as 125 Mb/s (see Fig. 8, inset). On the other hand, the single-mode holey VCSEL in Fig. 2(b) operating at 15 Gb/s benefits from the larger optical aperture, and thus smaller aperture size difference. The single-mode holey VCSELs generally exhibit shorter rise/fall time and wider large-signal bandwidth (>15 Gb/s modulation is not shown) than the single-mode PhC VCSELs. Note that one advantage of the holey VCSEL is to design single-mode VCSELs with

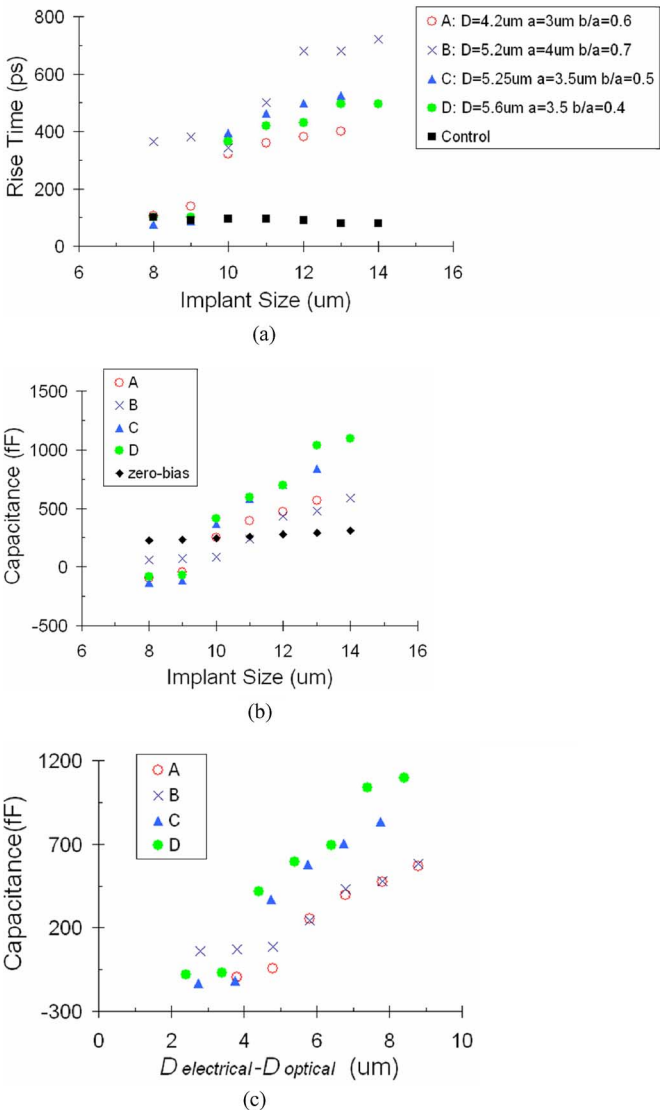

Fig. 9. (a) Measured rise time as a function of implant diameter for single-mode PhC VCSELs of four different designs, which are determined by the lattice spacing a and hole diameter b. Control VCSELs are with implant only and operate multimode. (b) Extracted lateral diffusion capacitance as a function of implant aperture diameter. (c) Extracted lateral diffusion capacitance as a function of diameter difference between implant and optical aperture.

relatively large optical apertures. Therefore, decreasing the aperture size difference improves the spatial overlap between the optical mode and laser gain, and will reduce the rise or fall transition time by reducing lateral carrier diffusion.

D. Design Rules

In order to optimize the design of high-speed single-mode PhC or holey VCSEL, it is valuable to obtain the optimal diameter for the electrical and optical aperture. Fig. 9(a) shows the rise time as a function of the implant aperture for four different single-mode PhC designs that produce an optical aperture varying from 4.2 to 5.6 μm. Note that the optical aperture size is determined by the PhC parameters a and b. Design B has the longest rise time due to its larger series resistance arising from

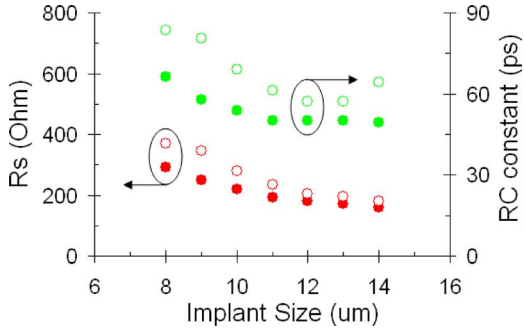

Fig. 10. Measured series resistance and zero-bias *RC* constant as a function of implant diameter for single-mode PhC VCSELs (open dot) and control VCSELs (solid dot). The PhC parameters for the single-mode VCSELs are $a = 3.5$ μm and $b/a = 0.4$. Control VCSELs are with implant only and operate multimode.

greater etched volume of its larger hole size. Similar single-mode VCSEL designs with large etched volume are found responsible for the large variation in their rise time, as shown in Fig. 7. The rise time for all four PhC VCSELs is greater than that calculated from the *RC* time constant determined at zero bias. The zero-bias *RC* time constant is calculated as the product of dc differential series resistance and zero-bias capacitance of the VCSEL. Fig. 9(b) and (c) shows the lateral diffusion capacitance extracted from dividing the difference between the measured and zero-bias *RC*-limited rise time by the series differential resistance R. The effective negative value of diffusion capacitance in Fig. 9(b) and (c) is attributed to the enhancement of the rising edge of the modulation pulse by the relaxation oscillation. As evident from Fig. 9(b) and (c), the diffusion capacitance decreases as the implant diameter and/or the aperture diameter difference becomes smaller. For an optimal design, the aperture diameter difference should be less than 4 μm to avoid excessive lateral diffusion capacitance and exacerbated electrical parasitics.

Increasing the optical diameter is constrained by the single-mode PhC or holey design, while decreasing the implant diameter is limited by implantation straggle and excessive high series resistance and increased junction heating. Fig. 10 plots the series resistance and zero-bias *RC* constant as a function of implant size for single-mode PhC VCSELs and multimode VCSELs with no etched pattern. The PhC VCSELs have higher series resistance due to the material removed from the etched holes. The optimal implant aperture diameter is $\sim$12 μm to achieve both small series resistance and zero-bias *RC* constant, which is consistent with the highest small-signal bandwidth measurements [6]. On the other hand, the scalability of the PhC or holey VCSEL permits single-mode operation with a larger optical aperture, yet it comes with the tradeoff of shallower etch depth and instability of optical confinement due to thermal fluctuation [10], [14].

The design rules for the high-speed single-mode PhC and holey VCSEL can be summarized: 1) the diameter difference between the implant and optical apertures should be $\leq$4 μm in order to avoid excessive lateral diffusion capacitance, and thus overall electrical parasitics; 2) the optimal implant aperture

diameter is $\sim$12 μm; and 3) the PhC structure with $b/a \leq 0.6$ is desired to avoid excessive series resistance and device heating.

IV. Conclusion

A PhC or holey wedge structure fabricated into implant-confined VCSELs can simultaneously stabilize the fundamental optical mode and achieve high-speed operation. In this paper, we demonstrated 12.5 Gb/s (and 15 Gb/s) operation of a single-mode implant-confined PhC (and holey) VCSEL. The fastest single-mode PhC VCSEL is limited to 12.5 Gb/s operation, due to an electrical parasitic effect from carrier diffusion induced by the large diameter difference between its implant and optical aperture. Moreover, it is observed that the spatial overlap between the optical mode and laser gain is of importance for high-speed large-signal operation, and it can be optimized by engineering the implant and optical apertures separately. A set of design rules can be extracted to provide the optimal sizing for the implant and optical apertures for high-speed single-mode index-guided VCSELs.

References

[1] F. Hopfer, A. Mutig, M. Kuntz, G. Fiol, D. Bimberg, N. N. Ledentsov, V. Shchukin, S. S. Mikhrin, I. L. Krestnikov, D. A. Livshits, A. R. Kovsh, N. D. Zakharov, and P. Werner, "Single-mode submonolayer quantum-dot vertical-cavity surface-emitting lasers with high modulation bandwidth," *Appl. Phys. Lett.*, vol. 89, pp. 141106-1–141106-3, 2006.

[2] Y. C. Chang, C. S. Wang, and L. A. Coldren, "High-efficiency, high-speed VCSELs with 35 Gb/s error-free operation," *Electron. Lett.*, vol. 43, no. 19, pp. 1022–1023, 2007.

[3] T. Anan, N. Suzuki, K. Yashiki, K. Fukatsu, H. Hatakeyama, T. Akagawa, and M. Tsuji, "High-speed 1.1-μm-range InGaAs VCSELs," in *Proc. Opt. Fiber Commun. Conf.*, San Diego, CA, Mar. 2008, pp. 1–3.

[4] R. H. Johnson and D. M. Kuchta, "30 Gb/s directly modulated 850 nm datacom VCSELs," presented at the Conf. Lasers Electro Opt., San Jose, CA, May 2008, Paper CPDB2.

[5] A. N. Al-Omari and K. L. Lear, "Polyimide-planarized vertical-cavity surface-emitting lasers with 17.0-GHz bandwidth," *IEEE Photon. Technol. Lett.*, vol. 16, no. 4, pp. 969–971, Apr. 2004.

[6] P. O. Leisher, C. Chen, J. D. Sulkin, M. S. B. Alias, K. A. M. Sharif, and K. D. Choquette, "High modulation bandwidth implant-confined photonic crystal vertical cavity surface emitting laser," *IEEE Photon. Technol. Lett.*, vol. 19, no. 19, pp. 1541–1543, Oct. 2007.

[7] T. Wipiejewski, D. B. Young, M. G. Peters, B. J. Thibeault, and L. A. Coldren, "Improved performance of vertical-cavity surface-emitting laser-diodes with Au-plated heat spreading later," *Electron. Lett.*, vol. 31, pp. 279–281, Feb. 1995.

[8] A. N. Al-Omari and K. L. Lear, "VCSELs with a self-aligned contact and copper-plated heatsink," *IEEE Photon. Technol. Lett.*, vol. 17, no. 9, pp. 1767–1769, Sep. 2005.

[9] P. O. Leisher, A. J. Danner, J. J. Raftery, Jr., D. F. Siriani, and K. D. Choquette, "Loss and index guiding in single-mode proton-implanted holey vertical-cavity surface-emitting lasers," *IEEE J. Quantum Electron.*, vol. 42, no. 10, pp. 1091–1096, Oct. 2006.

[10] N. Yokouchi, A. J. Danner, and K. D. Choquette, "Two-dimensional photonic crystal confined vertical-cavity surface-emitting lasers," *IEEE J. Sel. Topics Quantum Electron.*, vol. 9, no. 5, pp. 1439–1445, Sep./Oct. 2003.

[11] D. M. Kuchta, J. Gamelin, J. D. Walker, J. Lin, K. Y. Lau, and J. S. Smith, "Relative intensity noise of vertical cavity surface emitting lasers," *Appl. Phys. Lett.*, vol. 62, no. 11, pp. 1194–1196, Mar. 1993.

[12] L.-G. Zei, S. Ebers, J.-R. Kropp, and K. Petermann, "Noise performance of multimode VCSELs," *IEEE J. Quantum Electron.*, vol. 19, no. 6, pp. 884–892, Jun. 2001.

[13] K. Petermann, *Laser Diode Modulation and Noise*. Dordrecht, The Netherlands: Kluwer, 1988.

[14] P. O. Leisher, J. D. Sulkin, and K. D. Choquette, "Parametric study of proton implanted photonic crystal vertical-cavity surface-emitting lasers," *IEEE J. Sel. Topics Quantum Electron.*, vol. 13, no. 5, pp. 1290–1294, Oct./Nov. 2007.

Chen Chen (S'07) received the B.S. and M.S. degrees in electrical and computer engineering in 2004 and 2006, respectively, from the University of Illinois at Urbana-Champaign, Urbana, where he is currently working toward the Ph.D. degree in electrical and computer engineering.

His current research interests include design, fabrication, and characterization of vertical-cavity surface-emitting lasers and other novel optoelectronics devices with emphasis on their high-speed applications.

Paul O. Leisher (S'98–M'07) received the B.S. degree in electrical engineering from Bradley University, Peoria, IL, in 2002, and the M.S. and Ph.D. degrees in electrical and computer engineering from the University of Illinois at Urbana-Champaign, Urbana, in 2004 and 2007, respectively.

In 2007, he joined nLight Corporation, Vancouver, WA, where he is currently a Device Engineer. His current research interests include the design, fabrication, characterization, and analysis of semiconductor lasers and other photonic devices. He has authored or coauthored more than 50 technical journal papers and conference presentations.

Dr. Leisher is a member of the IEEE Lasers and Electro-Optics Society and the Optical Society of America.

Daniel M. Kuchta (S'85–M'86–SM'97) received the B.S., M.S., and Ph.D. degrees in electrical engineering and computer science from the University of California at Berkeley, Berkeley, in 1986, 1988, and 1992, respectively.

He is currently a Research Staff Member in the Communication Technology Department, IBM Thomas J. Watson Research Center, where he was engaged in research on high-speed vertical-cavity surface-emitting laser (VCSEL) characterization, multimode fiber links, and parallel fiber optic link research. He is the author or coauthor of more than 50 technical papers, and holds ten patents.

Kent D. Choquette (M'97–SM'02–F'03) received the B.S. degree in engineering physics and applied mathematics from the University of Colorado, Boulder, and the M.S. and Ph.D. degrees in materials science from the University of Wisconsin-Madison, Madison.

From 1990 to 1992, he was a Postdoctoral Fellow at AT&T Bell Laboratories, Murray Hill, NJ. He then joined Sandia National Laboratories, Albuquerque, NM, where he was a Principal Member of the Technical Staff from 1993 to 2000. In 2000, he became a Professor in the Department of Electrical and Computer Engineering, University of Illinois at Urbana-Champaign, Urbana, where he is with the Photonic Device Research Group, and is involved in the design, fabrication, characterization, and applications of vertical-cavity surface-emitting lasers (VCSELs), photonic crystal light sources, nanofabrication technologies, and hybrid integration techniques for photonic devices. He has authored or coauthored more than 200 technical publications and three book chapters, and has presented numerous invited talks and tutorials.

Prof. Choquette was an Associate Editor of the IEEE JOURNAL OF QUANTUM ELECTRONICS and the IEEE PHOTONIC TECHNOLOGY LETTERS. He was a Guest Editor of the IEEE JOURNAL OF SELECTED TOPICS IN QUANTUM ELECTRONICS. From 2000 to 2002, he was an IEEE/Lasers and Electro-Optics Society (LEOS) Distinguished Lecturer. He was awarded the 2008 IEEE/LEOS Engineering Achievement Award. He is a Fellow of the Optical Society of America and the International Society for Optical Engineers (SPIE).